Transient Dynamic Crack Analysis in Decagonal Quasicrystal

Jan Sladek[1,*], Vladimir Sladek[1], Slavomir Krahulec[1], Chuanzeng Zhang[2], Michael Wünsche[2]

[1] Institute of Construction and Architecture, Slovak Academy of Sciences, 84503 Bratislava, Slovakia
[2] Department of Civil Engineering, University of Siegen, D-57068 Siegen, Germany
* Corresponding author: jan.sladek@savba.sk

Abstract: A meshless method based on the local Petrov-Galerkin approach is proposed to solve initial-boundary value crack problems in decagonal quasicrystals. These quasicrystals belong to the class of two-dimensional quasicrystals, where the atomic arrangement is quasiperiodic in a plane, and periodic in the perpendicular direction. The ten-fold symmetries occur in these quasicrystals. The two-dimensional (2-d) crack problem is represented by a coupling of phonon and phason displacements. Both stationary governing equations and dynamic equations represented by the Bak model with oscillations for phason are analyzed here. Nodal points are spread on the analyzed domain, and each node is surrounded by a small circle for simplicity. The spatial variation of the phonon and phason displacements is approximated by the Moving Least-Squares (MLS) scheme. After performing the spatial integrations, one obtains a system of ordinary differential equations for certain nodal unknowns. That system is solved numerically by the Houbolt finite-difference scheme as a time-stepping method.

Keywords: Meshless local Petrov-Galerkin method (MLPG), phonon, phason, intensity factors

1. Introduction

Qusicrystals discovered in 1984 combine aperiodic long-range positional order with noncrystallographic rotational symmetry [1]. Decagonal quasicrystals (QC) belong to the class of two-dimensional quasicrystals, where the atomic arrangement is quasiperiodic in a plane, and periodic in the third direction. The problem can be decomposed into plane and anti-plane elasticity. Here, we consider only the plane elasticity, because the anti-plane elasticity is a classical one.

Experimental observations [2] have shown that quasicrystals are brittle. Therefore, to understand the effect of cracks on the mechanical behaviour of a quasicrystal, the crack analysis of quasicrystals, including the determination of the stress intensity factors, the elastic field, the strain energy release rate and so on, is a prerequisite. Many crack investigations in the QC are focused on Griffith cracks in an infinite body, where analytical solutions are available for one and two-dimensional quasicrystals [3-6]. Elastodynamics of quasicrystals brings some additional problems. A unique opinion on governing equations for the phason field is missing. According to Bak [7] the phason describes particular structure disorders in qusicrystals, and it can be formulated in a six-dimensional space. Since there are six continuous symmetries, there exist six hydrodynamic vibration modes. Then, phonons and phasons play similar roles in the dynamics and both fields should be described by similar governing equations, namely the balance of momentum. Lubensky and his students [8] were thinking that the phason field should be described by a diffusion equation with very a large diffusion time. According to them, phasons are insensitive to spatial translations and phason modes represent the relative motion of the constituent density waves. Rochal and

Lorman [9] suggested the minimal model of the phonon-phason dynamics in quasicrystals to reconcile contradictions between Bak´s and Lubensky´s arguments. In literature, analyses of dynamic crack problems are very seldom [10-12].

The purpose of this paper is to develop a reliable computational method for a general crack problem in quasicrystals with a finite size. Up to date we have practically only analytical solutions for simple boundary value problems of elasticity for quasicrystals. However, there are some limitations to apply analytical approaches for complicated boundary value problems. The finite difference method has been applied to elasto-hydrodynamics problems by Fan [12]. The basic equations for the finite element formulation can be found in the Fan`s book too. Meshless methods for solving PDE in physics and engineering sciences are a powerful new alternative to the traditional mesh-based techniques. Focusing only on nodes or points instead of elements used in the conventional FEM, meshless approaches have certain advantages. The meshless local Petrov-Galerkin (MLPG) method is a fundamental base for the derivation of many meshless formulations, since trial and test functions can be chosen from different functional spaces. The MLPG method with a Heaviside step function as the test functions has been successfully applied to multi-field coupled and crack problems [13,14].

In the present paper, the MLPG is applied to crack analysis in decagonal quasicrystals under static and transient dynamic loads. The MLPG formulation is developed for the Bak`s model. The coupled governing partial differential equations are satisfied in a weak-form on small fictitious subdomains. Nodal points are introduced and spread on the analyzed domain and each node is surrounded by a small circle for simplicity, but without loss of generality. The spatial variations of the phonon and phason displacements are approximated by the Moving Least-Squares (MLS) scheme. After performing the spatial MLS approximation, a system of ordinary differential equations for certain nodal unknowns is obtained. Then, the system of the ordinary differential equations of the second order resulting from the equations of motion is solved by the Houbolt finite-difference scheme [15] as a time-stepping method.

2. Local integral equations

Two displacement fields named phonon and phason displacements are used for the deformation theory of quasicrystals [12]. The generalized Hooke`s law for plane elasticity of decagonal QC is given as

$$\sigma_{11} = c_{11}\varepsilon_{11} + c_{12}\varepsilon_{22} + R(w_{11} + w_{22}), \qquad \sigma_{22} = c_{12}\varepsilon_{11} + c_{22}\varepsilon_{22} - R(w_{11} + w_{22}),$$

$$\sigma_{12} = \sigma_{21} = 2c_{66}\varepsilon_{12} + R(w_{21} - w_{12}),$$

$$H_{11} = K_1 w_{11} + K_2 w_{22} + R(\varepsilon_{11} - \varepsilon_{22}), \qquad H_{22} = K_1 w_{22} + K_2 w_{11} + R(\varepsilon_{11} - \varepsilon_{22}),$$

$$H_{12} = K_1 w_{12} - K_2 w_{21} - 2R\varepsilon_{12}, \qquad H_{21} = K_1 w_{21} - K_2 w_{12} + 2R\varepsilon_{12}, \tag{1}$$

where ε_{ij} and σ_{ij} correspond to the phonon strain and stress tensor, and w_{ij} and H_{ij} denote the

phason strain and stress tensor, respectively. Symbols c_{ij} , R and K_i denote phonon elastic constants, phonon-phason coupling parameter and phason elastic constants, respectively. The phonon and phason strains are defined as

$$\varepsilon_{ij}(\mathbf{x}) = \frac{1}{2}\left(u_{i,j} + u_{j,i}\right), \tag{2}$$

$$w_{ij}(\mathbf{x}) = w_{i,j}(\mathbf{x}), \tag{3}$$

where $u_i(\mathbf{x})$ and $w_i(\mathbf{x})$ are the phonon and phason displacements, respectively. The phonon field describes the mechanical displacements of the crystal system, and the phason field represents the atom arrangement along the quasiperiodic direction. The phonon strains are the same as in classical elasticity and they are symmetric. However, the phason strains are new physical quantities used only in quasi-crystal elasticity and they are asymmetric.

According to Bak`s model [7] the phason structure disorders are realized by fluctuations in quasicrystals. The balance of momentum is valid for phonon deformation and similarly for phason oscillations too. Then, the model is described by following governing equations:

$$\sigma_{ij,j}(\mathbf{x},\tau) + X_i(\mathbf{x},\tau) = \rho \ddot{u}_i(\mathbf{x},\tau), \tag{4}$$

$$H_{ij,j}(\mathbf{x},\tau) + g_i(\mathbf{x},\tau) = \rho \ddot{w}_i(\mathbf{x},\tau), \tag{5}$$

where $\ddot{u}_i$, $\ddot{w}_i$, ρ, X_i and g_i denote the acceleration of the phonon and phason displacements, the mass density, and the body force vectors, respectively. Both governing equations have mathematically a similar structure.

The MLPG method constructs a weak-form over the local fictitious subdomains such as Ω_s, which is a small region taken for each node inside the global domain [16]. The local subdomains could be of any geometrical shape and size. In the present paper, the local subdomains are taken to be of a circular shape for simplicity. The local weak-form of the governing equations (4) and (5) can be written as

$$\int_{\Omega_s} \left[\sigma_{ij,j}(\mathbf{x},\tau) - \rho \ddot{u}_i(\mathbf{x},\tau) + X_i(\mathbf{x},\tau)\right] u_{ik}^*(\mathbf{x})\, d\Omega = 0, \tag{6}$$

$$\int_{\Omega_s} \left[H_{ij,j}(\mathbf{x},\tau) - \rho \ddot{w}_i(\mathbf{x},\tau) + g_i(\mathbf{x},\tau)\right] u_{ik}^*(\mathbf{x})\, d\Omega = 0, \tag{7}$$

where $u_{ik}^*(\mathbf{x})$ is a test function. Applying the Gauss divergence theorem to the first domain integrals in both equations one gets

$$\int_{\partial\Omega_s} \sigma_{ij}(\mathbf{x},t) n_j(\mathbf{x}) u_{ik}^*(\mathbf{x}) d\Gamma - \int_{\Omega_s} \sigma_{ij}(\mathbf{x},t) u_{ik,j}^*(\mathbf{x}) d\Omega + \int_{\Omega_s} \left[-\rho \ddot{u}_i(\mathbf{x},t) + X_i(\mathbf{x},t)\right] u_{ik}^*(\mathbf{x}) d\Omega = 0, \tag{8}$$

$$\int_{\partial\Omega_s} H_{ij}(\mathbf{x},t) n_j(\mathbf{x}) u_{ik}^*(\mathbf{x}) d\Gamma - \int_{\Omega_s} H_{ij}(\mathbf{x},t) u_{ik,j}^*(\mathbf{x}) d\Omega + \int_{\Omega_s} \left[-\rho \ddot{w}_i(\mathbf{x},t) + g_i(\mathbf{x},t)\right] u_{ik}^*(\mathbf{x}) d\Omega = 0, \tag{9}$$

where $\partial\Omega_s$ is the boundary of the local subdomain which consists of three parts $\partial\Omega_s = L_s \cup \Gamma_{st} \cup \Gamma_{su}$ [16]. Here, L_s is the local boundary that is totally inside the global domain, Γ_{st} is the part of the local boundary which coincides with the global traction boundary, i.e., $\Gamma_{st} = \partial\Omega_s \cap \Gamma_t$, and similarly Γ_{su} is the part of the local boundary that coincides with the global displacement boundary, i.e., $\Gamma_{su} = \partial\Omega_s \cap \Gamma_u$.

By choosing a Heaviside step function as the test function $u_{ik}^*(\mathbf{x})$ in each subdomain the local weak-forms (6) and (7) are converted into the following local integral equations

$$\int_{L_s+\Gamma_{su}} t_i(\mathbf{x},\tau)d\Gamma - \int_{\Omega_s} \rho\ddot{u}_i(\mathbf{x},\tau)d\Omega = -\int_{\Gamma_{st}} \bar{t}_i(\mathbf{x},\tau)d\Gamma - \int_{\Omega_s} X_i(\mathbf{x},\tau)d\Omega, \tag{10}$$

$$\int_{L_s+\Gamma_{su}} h_i(\mathbf{x},\tau)d\Gamma - \int_{\Omega_s} \rho\ddot{w}_i(\mathbf{x},\tau)d\Omega = -\int_{\Gamma_{st}} \bar{h}_i(\mathbf{x},\tau)d\Gamma - \int_{\Omega_s} g_i(\mathbf{x},\tau)d\Omega. \tag{11}$$

The expressions for the traction and the generalized traction vectors result from the constitutive equations and are given as

$$t_i(\mathbf{x},\tau) = \left[c_{ijkl}(\mathbf{x})u_{k,l}(\mathbf{x},\tau) + R_{ijkl}(\mathbf{x})w_{k,l}(\mathbf{x},\tau) \right] n_j(\mathbf{x}), \tag{12}$$

$$h_i(\mathbf{x},\tau) = \left[K_{ijkl}(\mathbf{x})w_{k,l}(\mathbf{x},\tau) + R_{ijkl}(\mathbf{x})u_{k,l}(\mathbf{x},\tau) \right] n_j(\mathbf{x}), \tag{13}$$

where $n_j(\mathbf{x})$ is the unit outward normal vector to the boundary $\partial\Omega_s$.

The trial functions are chosen to be the MLS approximations by using a number of nodes spreading over the domain of influence. The approximated functions for the phonon and phason displacements can be written as [16]

$$\mathbf{u}^h(\mathbf{x},\tau) = \mathbf{\Phi}^T(\mathbf{x}) \cdot \hat{\mathbf{u}} = \sum_{a=1}^{n} \phi^a(\mathbf{x})\mathbf{u}^a(\tau), \tag{14}$$

$$\mathbf{w}^h(\mathbf{x},\tau) = \sum_{a=1}^{n} \phi^a(\mathbf{x})\hat{\mathbf{w}}^a(\tau), \tag{15}$$

where the nodal values $\hat{\mathbf{u}}^a(\tau) = \left(u_1^a(\tau),\, u_2^a(\tau)\right)^T$ and $\hat{\mathbf{w}}^a(\tau) = \left(w_1^a(\tau),\, w_2^a(\tau)\right)^T$ are fictitious parameters for the phonon and phason displacements, respectively, and $\phi^a(\mathbf{x})$ is the shape function associated with the node *a*. The number of nodes *n* used for the approximation is determined by the weight function $m^a(\mathbf{x})$. A 4th order spline-type weight function [16] is applied in the present work.

Then, the traction vector $t_i(\mathbf{x},\tau)$ at a boundary point $\mathbf{x}\in\partial\Omega_s$ is approximated in terms of the same nodal values $\hat{\mathbf{u}}^a(\tau)$ and $\hat{\mathbf{w}}^a(\tau)$ as

$$\mathbf{t}^h(\mathbf{x},\tau)=\mathbf{N}(\mathbf{x})\mathbf{C}\sum_{a=1}^{n}\mathbf{B}^a(\mathbf{x})\hat{\mathbf{u}}^a(\tau)+\mathbf{N}(\mathbf{x})\mathbf{R}\sum_{a=1}^{n}\mathbf{B}_w^a(\mathbf{x})\mathbf{w}^a(\tau), \tag{16}$$

where **N(x)** is related to the normal vector **n(x)** on $\partial\Omega_s$ and the matrices $\mathbf{B}^a$ and $\mathbf{B}_w^a$ are represented by the gradients of the shape functions with

$$\mathbf{N}(\mathbf{x})=\begin{bmatrix} n_1 & 0 & n_2\\ 0 & n_2 & n_1\end{bmatrix},\qquad \mathbf{B}^a(\mathbf{x})=\begin{bmatrix}\phi^a_{,1} & 0\\ 0 & \phi^a_{,2}\\ \phi^a_{,2} & \phi^a_{,1}\end{bmatrix},\qquad \mathbf{B}_w^a(\mathbf{x})=\begin{bmatrix}\phi^a_{,1} & 0\\ 0 & \phi^a_{,2}\\ \phi^a_{,2} & -\phi^a_{,1}\end{bmatrix},$$

and the material matrices

$$\mathbf{C}=\begin{bmatrix} c_{11} & c_{12} & 0\\ c_{12} & c_{22} & 0\\ 0 & 0 & c_{66}\end{bmatrix},\qquad \mathbf{R}=\begin{bmatrix} R & R & 0\\ -R & -R & 0\\ 0 & 0 & -R\end{bmatrix}.$$

Similarly the generalized traction vector $h_i(\mathbf{x},\tau)$ can be approximated by

$$\mathbf{h}^h(\mathbf{x},\tau)=\mathbf{N}_h(\mathbf{x})\mathbf{R}_h\sum_{a=1}^{n}\mathbf{B}^a(\mathbf{x})\hat{\mathbf{u}}^a(\tau)+\mathbf{N}_h(\mathbf{x})\mathbf{K}\sum_{a=1}^{n}\mathbf{B}_{hw}^a(\mathbf{x})\mathbf{w}^a(\tau), \tag{17}$$

where

$$\mathbf{N}_h(\mathbf{x})=\begin{bmatrix} n_1 & 0 & n_2 & 0\\ 0 & n_2 & 0 & n_1\end{bmatrix},\qquad \mathbf{K}=\begin{bmatrix} K_1 & K_2 & 0 & 0\\ K_2 & K_1 & 0 & 0\\ 0 & 0 & K_1 & -K_2\\ 0 & 0 & -K_2 & K_1\end{bmatrix},$$

$$\mathbf{B}_{hw}^a(\mathbf{x})=\begin{bmatrix}\phi^a_{,1} & 0\\ 0 & \phi^a_{,2}\\ \phi^a_{,2} & 0\\ 0 & \phi^a_{,1}\end{bmatrix},\qquad R_h=\begin{bmatrix} R & -R & 0\\ R & -R & 0\\ 0 & 0 & -R\\ 0 & 0 & R\end{bmatrix}.$$

Satisfying the essential boundary conditions and making use of the approximation formulae (14) and (15) one obtains the discretized form of these boundary conditions as

$$\sum_{a=1}^{n}\phi^a(\zeta)\hat{\mathbf{u}}^a(\tau)=\bar{\mathbf{u}}(\zeta,\tau), \tag{18}$$

$$\sum_{a=1}^{n}\phi^a(\zeta)\mathbf{w}^a(\tau)=\bar{\mathbf{w}}(\zeta,\tau),\qquad \text{for}\quad \zeta\in\Gamma_u. \tag{19}$$

Furthermore, in view of the MLS-approximations (16) and (17) for the unknown quantities in the local integral equations (10) and (11), we obtain their discretized forms as

$$\sum_{a=1}^{n}\left[\left(\int_{L_s+\Gamma_{st}}\mathbf{N}(\mathbf{x})\mathbf{C}\mathbf{B}^a(\mathbf{x})d\Gamma\right)\dot{\hat{\mathbf{u}}}^a(\tau)-\left(\int_{\Omega_s}\rho(\mathbf{x})\phi^a d\Omega\right)\ddot{\hat{\mathbf{u}}}^a(\tau)\right]+$$

$$+\sum_{a=1}^{n}\left(\int_{L_s+\Gamma_{st}}\mathbf{N}(\mathbf{x})\mathbf{R}\mathbf{B}_w^a(\mathbf{x})d\Gamma\right)\hat{\mathbf{w}}^a(\tau)\;=-\int_{\Gamma_{st}}\bar{\mathbf{t}}(\mathbf{x},\tau)d\Gamma-\int_{\Omega_s}\mathbf{X}(\mathbf{x},\tau)d\Omega\,, \tag{20}$$

$$\sum_{a=1}^{n}\left(\int_{L_s+\Gamma_{st}}\mathbf{N}_h(\mathbf{x})\mathbf{R}_h\mathbf{B}^a(\mathbf{x})d\Gamma\right)\dot{\hat{\mathbf{u}}}^a(\tau)\;-\sum_{a=1}^{n}\left(\int_{L_s+\Gamma_{st}}\mathbf{N}_h(\mathbf{x})\mathbf{K}\mathbf{B}_{hw}^a(\mathbf{x})d\Gamma\right)\mathbf{w}^a(\tau)-$$

$$-\sum_{a=1}^{n}\left(\int_{\Omega_s}\rho(\mathbf{x})\phi^a d\Omega\right)\ddot{\mathbf{w}}^a(\tau)=-\int_{\Gamma_{st}}\bar{\mathbf{h}}(\mathbf{x},\tau)d\Gamma+\int_{\Omega_s}\mathbf{g}(\mathbf{x},\tau)d\Omega\,, \tag{21}$$

which are considered on the sub-domains adjacent to the interior nodes as well as to the boundary nodes on Γ_{st}.

Collecting the discretized local integral equations together with the discretized boundary conditions for the phonon and phason displacements results in a complete system of ordinary differential equations which can be rearranged in such a way that all known quantities are on the r.h.s. Thus, in matrix form the system becomes

$$\mathbf{A}\ddot{\mathbf{x}}+\mathbf{C}\mathbf{x}=\mathbf{Y}\,. \tag{22}$$

There are many time integration procedures for the solution of this system of ordinary differential equations. In the present work, the Houbolt method is applied [15].

3. Computation of stress intensity factors

It can be proved that both phonon and phason stresses exhibit the same singularity $r^{-1/2}$, where r is the radial coordinate with origin at the crack-tip [17]. Neglecting higher-order infinitesimal terms in the analytical solution, one can obtain the asymptotic expression of stresses at the crack-tip vicinity proportional to $r^{-1/2}$. For the mode-I crack under a pure phonon load we have the following asymptotic stresses in polar coordinate system [11]:

$$\sigma_{11}(r,\theta)=\frac{K_I^{\parallel}}{\sqrt{2\pi r}}\cos\frac{1}{2}\theta\left(1-\sin\frac{1}{2}\theta\sin\frac{3}{2}\theta\right),$$

$$\sigma_{22}(r,\theta)=\frac{K_I^{\parallel}}{\sqrt{2\pi r}}\cos\frac{1}{2}\theta\left(1+\sin\frac{1}{2}\theta\sin\frac{3}{2}\theta\right),$$

$$\sigma_{12}(r,\theta)=\sigma_{21}(r,\theta)=\frac{K_I^{\parallel}}{\sqrt{2\pi r}}\cos\frac{1}{2}\theta\cos\frac{3}{2}\theta\,, \tag{23}$$

$$H_{11}(r,\theta)=-\frac{d_{21}K_I^{\parallel}}{\sqrt{2\pi r}}\sin\theta\left(2\sin\frac{3}{2}\theta+\frac{3}{2}\sin\theta\cos\frac{5}{2}\theta\right),$$

$$H_{22}(r,\theta)=\frac{d_{21}K_I^{\parallel}}{\sqrt{2\pi r}}\frac{3}{2}\sin^2\theta\cos\frac{5}{2}\theta\,,$$

$$H_{12}(r,\theta)=-\frac{d_{21}K_I^{\parallel}}{\sqrt{2\pi r}}\frac{3}{2}\sin^2\theta\sin\frac{5}{2}\theta\,,$$

$$H_{21}(r,\theta)=\frac{d_{21}K_I^{\parallel}}{\sqrt{2\pi r}}\sin\theta\left(2\cos\frac{3}{2}\theta-\frac{3}{2}\sin\theta\sin\frac{5}{2}\theta\right), \tag{24}$$

where

$$d_{21}=\frac{R\left(K_1-K_2\right)}{4\left(MK_1-R^2\right)},$$

$$K_I^{\mathrm{P}}=\lim_{r\to 0}\sqrt{2\pi r}\,\sigma_{22}(r,0)\,, \tag{25}$$

and $M=(c_{11}-c_{12})/2$.

4. Numerical examples

In the first example a straight central crack in a finite quasicrystal strip under a pure phonon load is analyzed (Fig. 1). The strip is subjected to a stationary or impact mechanical load with Heaviside time variation and the intensity $\sigma_0=1Pa$ on the top side of the strip. The material coefficients of the strip correspond to Al-Ni-Co quasicrystal and they are given by

$c_{11}=L+2M=23.43\cdot10^{10}\,Nm^{-2}$, $c_{12}=L=5.74\cdot10^{10}\,Nm^{-2}$, $K_1=12.2\cdot10^{10}\,Nm^{-2}$,

$K_2=2.4\cdot10^{10}\,Nm^{-2}$, $\rho=4180\,kg/m^3$, $\Gamma_w=4.8\cdot10^{-19}\,m^3s/kg$.

The crack-length $2a=1.0m$, strip width ratio $a/w=0.4$, and strip-height $h=1.2w$ are considered. Due to the symmetry of the problem with respect to the crack-line as well as vertical central line, only a quarter of the specimen is numerically analyzed. Both phonon and phason displacements in the quarter of the specimen are approximated by using 930 (31x30) nodes equidistantly distributed.

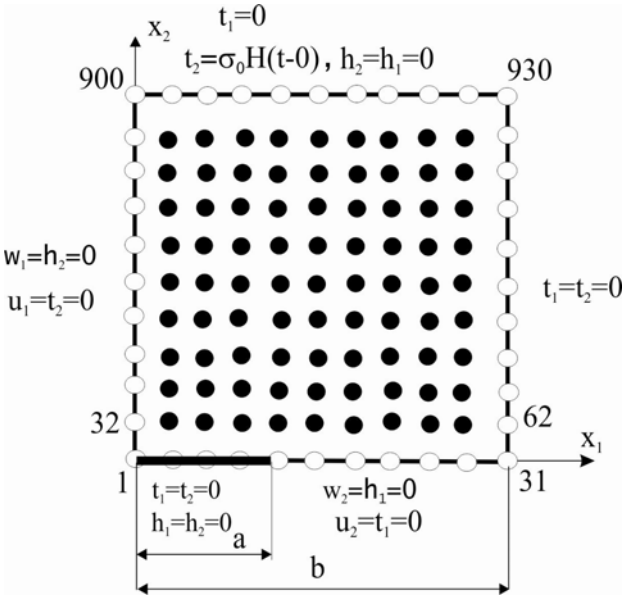

Figure 1. Central crack in a finite homogeneous strip

Numerical results for the phonon displacement u_2 along the crack-face for various coupling parameter R are given in Fig. 2. For a vanishing coupling parameter R/M = 0, we obtain phonon displacements corresponding to conventional elasticity. One can observe a good agreement between the FEM and present MLPG results. The FEM results have been obtained by the COMSOL code with 576 quadrilateral elements. One can observe that the phonon crack-opening-displacements increase with increasing value of the coupling parameter. The stress intensity factor (SIF) is computed by using equation (25) and the extrapolation technique from stresses ahead of the crack-tip with finite distances. The normalized SIF $K_I^{\mathrm{P}}/\sigma_0\sqrt{\pi a}$ is increasing from 1.139 at R/M=0 to 1.323 at R/M=0.5.

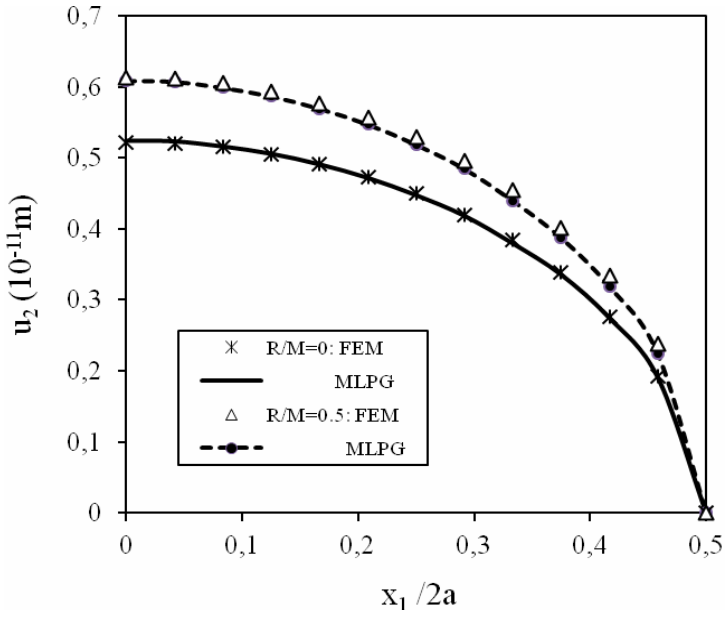

Figure 2. Variations of the phonon crack displacement with the normalized coordinate $x_1/2a$

In the next example, we analyze the same cracked strip under an impact load with Heaviside time variation $\sigma_0 H(t-0)$. The normalized SIF is compared with the FEM results in Fig. 3 for R/M=0.5 . The time variable is normalized as $c_L \tau / h$, where $c_L = \sqrt{c_{11}/\rho}$ is the velocity of longitudinal wave. One can observe again a good agreement of the FEM and MLPG results. Only some differences appear at larger time instants.

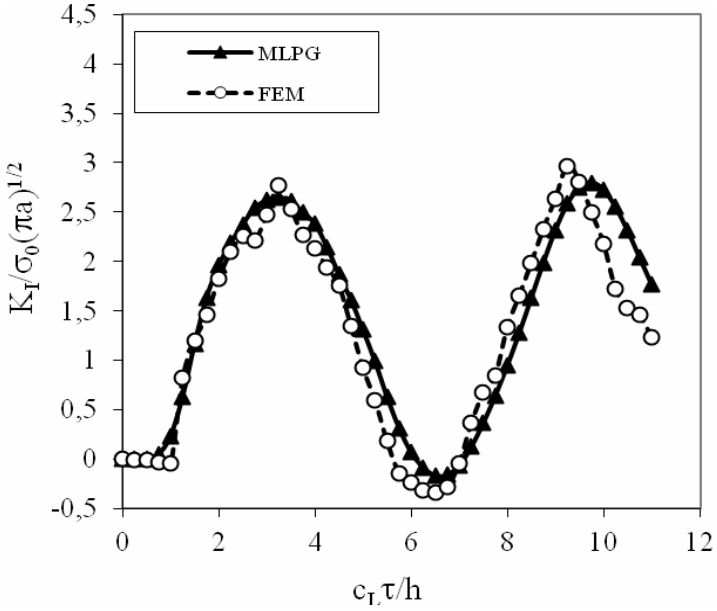

Figure 3. Temporal variation of the normalized SIF for the central crack in a strip under an impact load

Acknowledgements

The authors gratefully acknowledge the supports by the Slovak Science and Technology Assistance Agency registered under number APVV-0014-10, the Slovak Grant Agency VEGA-2/0011/13, and the German Research Foundation (DFG, Project-No. ZH 15/23-1).

References

[1] D. Shechtman, I. Blech, D. Gratias, J.W. Cahn, Metallic phase with long-range orientational order and no translational symmetry. Phys Rev Lett, 53 (1984) 1951–1953.
[2] C.Z. Hu, W.Z. Yang, R.H. Wang, Symmetry and physical properties of quasicrystals. Advanced Physics 17 (1997) 345-376.
[3] T.Y. Fan, Y.W. Mai, Elasticity theory, fracture mechanics and some relevant thermal properties of quasicrystal materials. Applied Mechanics Review 57 (2004) 325-344.
[4] W.M. Zhou, T.Y. Fan, Plane elasticity problem of two-dimensional octagonal quasicrystal and crack problem. Chinese Physics 10 (2001) 743-747.
[5] Y.C. Guo, T.Y. Fan, A mode-II Griffith crack in decagonal quasicrystals. Appl Math Mechanics 22 (2001) 1311-1317.
[6] L.H. Li, T.Y. Fan, Complex variable function method for solving Griffith crack in an icosahedral quasicrystal. Science in China G51 (2008) 773-780.

[7] P. Bak, Phenomenological theory of icosahedral incommensurate (quasiperiodic) order in Mn-Al alloys. Phys Rev Lett 54 (1985) 1517-1519.
[8] T.C. Lubensky, S. Ramaswamy, J. Joner, Hydrodynamics of icosahedral quasicrystals. Phys Rev B 32 (1985) 7444-7452.
[9] S.B. Rochal, V.L. Lorman, Minimal model of the phonon-phason dynamics on icosahedral quasicrystals and its application for the problem of internal friction in the Ni-AlPdMn alloys. Phys Rev B 66 (2002) 144204.
[10] A.Y. Zhu, T.Y. Fan, Dynamic crack propagation in a decagonal Al-Ni-Co quasicrystal. J Phys: Condens Matter 20 (2008) 295217.
[11] T.Y. Fan, Z.Y. Tang, W.Q. Chen, Theory of linear, nonlinear and dynamic fracture for quasicrystals. Engn Fracture Mech 82 (2012) 185-194.
[12] T.Y. Fan, Mathematical Theory of Elasticity of Quasicrystals and its Applications, Springer, Beijing, 2011.
[13] J. Sladek, V. Sladek, Ch. Zhang, M. Wünsche, Crack analysis in piezoelectric solids with energetically consistent boundary conditions by the MLPG. CMES-Computer Modelling in Engineering & Sciences 68 (2010) 185-220.
[14] J. Sladek, V. Sladek, S. Krahulec, E. Pan, Enhancement of the magnetoelectric coefficient in functionally graded multiferroic composites. J Intell Mat Syst Struct 23 (2012) 1644-1653.
[15] J.C. Houbolt, A recurrence matrix solution for the dynamic response of elastic aircraft. Journal of Aeronautical Sciences 17 (1950) 371-376.
[16] S.N. Atluri, The Meshless Method, (MLPG) for Domain & BIE Discretizations, Tech Science Press, Encino, 2004.
[17] X.F. Li, T.Y. Fan, Y.F. Sun, A decagonal quasicrystal with a Griffith crack. Philosophical Magazine A 79 (1999) 1943-1952.